Heterogeneous Fenton-like degradation of synthetic dye using optimized layered double hydroxide

MANAA Zoubir[1]; CHEBLI Derradji[2]; BOUGUETTOUCHA AbdAllah[3]

[1] Department of Chemical process Engineering, Laboratory of Chemical Process Engineering, faculty of technology, university of Ferhat Abbes Setif-1, 19000 Setif Algeria, email: manaa13@yahoo.fr

[2] Department of Chemical process Engineering, Laboratory of Chemical Process Engineering, faculty of technology, university of Ferhat Abbes Setif-1, 19000 Setif Algeria, email: abdallah.bouguettoucha@univ-setif.dz

[3] Department of Chemical process Engineering, Laboratory of Chemical Process Engineering, faculty of technology, university of Ferhat Abbes Setif-1, 19000 Setif Algeria, email: derradji.chebli@yahoo.fr

Abstract

The present study concerns the synthesis and optimization of layered double hydroxide and their derivatives containing two transition metals, namely iron and copper, which have an important effect in heterogeneous Fenton oxidation by a classical method of a co-precipitation followed by a calcination. The use of experimental design of mixture is to optimize the LDH ratio component. The material was characterized by different methods such as, XRD, SEM, IR, Particles size distribution and UV-DRS. The degradation of the synthetic dye patent blue v was investigated by studying the different effects of parameters such as pH, dye initial concentration, H_2O_2 dose and photocatalyst loading. The catalytic reaction showed a good performance of oxidation of the dye in a wide range of pH particularly in natural pH. The catalyst kept its activity after several uses, demonstrating its stability and its promising long-term application in the treatment of wastewaters.

Keywords**:** *heterogeneous Fenton-like; layered double hydroxide; degradation; synthetic dye; catalyst stability.*

I. Introduction

In recent decades, the pollution of the aquatic environment by the massive presence of persistent synthetic dye in industrial wastewater effluents is a serious environmental problem. Contamination of groundwater or surface water with these products can be of significant threats to water resources and public health. More than 700000 tons of approximately 10000 types of dyes and pigments are produced in the word per year. About 20% from this amount is transported by the industrial effluents [1] into the environment mainly as a result of inefficient dyeing processes [2].

Blue Patent is an acidic dye commonly used for a wide range of applications in cosmetics, textiles, detergents and also as a food additive [1]. In Algeria, BPv is authorized as a food colouring substance (E133) with a quantitative limit of (50-500) $mg.kg^{-1}$ [3]. In Europe, the BP dye also known as Blue Acid 3 is authorized under the code of E133 in the food industry with a concentration not exceeding 15 mg kg^{-1}, whereas for cosmetics there is no limiting amount. Unlike Europe PB is not authorized for usage in food in USA, Australia, Canada, Japan, and New Zealand [4].

Several physical, chemical and biological processes have been developed to eliminate or destroy these pollutants, such as conventional processes, coagulation and flocculation, adsorption, biological treatment, membrane separation, etc. However, many types of serious toxic pollutants such as BPv are resistant to such treatment processes and the rate of degradation is very low [5]. Also the adsorption processes are sufficient to transfer the form of the pollutant from the water to the solid state without any destruction [6].

Advanced oxidation processes (AOPs) may be the efficient way for the treatment of industrial

wastewaters. They are based on the generation of the most powerful oxidant, the hydroxide radical [7]. The highly efficient reaction offers a cost-effective source of hydroxyl radicals, easy to use and to maintain. The Fenton oxidation of organic compounds in water is one of the most well known reactions among oxidation reactions catalyzed by metal [8]. The main disadvantage of this process is the fact that soluble iron, added as a catalyst, cannot be reused in the process and may cause additional water pollution. Undesirable iron sludge is generated, which requires an appropriate treatment and disposal [9]. To avoid the precipitation of dissolved iron, heterogeneous systems have been prepared which use iron-based catalysts, or other transition metals such as Cu, Ag, Zn, etc.

In this work, synthetic clay called layered double hydroxide or hydrotalcite-like, was used as a heterogeneous photocatalyst. This material contains two transition metals iron and copper and its derivatives are obtained by calcination in the electric muffle. The optimum composition ratio of this LDH was determined by an experimental design mixture.

II. Experimental

II.1 Materials

Blue Patent v abbreviated as BPv with the formulae ($C_{27}H_{31}N_2NaO_7S_2$) was purchased from Panreac with purity > 98% w/w. The aqueous solution of BPv was prepared by dissolving a 50 mg in 1000 ml of deionised water under stirring for sufficient time at room temperature; the solution was stored in dark. The used chemical reagents: $MgCl_2 \cdot 6H_2O$ (purity > 99%), $CuCl_2 \cdot 2H_2O$ (purity > 99%), $FeCl_3 \cdot 6H_2O$ (purity > 97%), Na_2CO_3, NaOH and HCl were all of analytical grade and were purchased from Panreac. They were also dissolved in the deionised water.

II.2 Catalyst preparation

An experimental design is a statistical approach that minimizes the number of tests to obtain reliable results that reflect the actual variation of the studied phenomenon according to its various parameters. Among the experimental designs used, the mixture scheme applied for this study aims to translate the variation of a response as a function of the constituents of the mixture by the relation $Y = f(Xi)$ with $\sum Xi = 1$ and i varies between 1 and k (k is the total number of factors).

MgCuFe-CO_3 LDH synthetic clay was prepared by a co-precipitation method widely described in the literature [10-12]. Aqueous solutions of metal chloride were dissolved in 250 ml of deionised water and precipitated dropwise over 2 hours with the solution of Na_2CO_3 0.5M and NaOH 1M, with different Mg^{2+}:Cu^{2+}:Fe^{3+} molar ratio and the total molar cations amount $n_{Mg} + n_{Cu} + n_{Fe} = 1$ mol. The obtained solids were denoted respectively Mi, i=1 to 7 as shown in the following table:

Table.1 matrix ratio component

Matrix/composition	Mg^{2+}	Cu^{2+}	Fe^{3+}
M1	0.45	0.1	0.45
M2	0.45	0.45	0.1
M3	0.1	0.8	0.1
M4	0.33	0.33	0.33
M5	0.8	0.1	0.1
M6	0.1	0.1	0.8
M7	0.1	0.45	0.45

During the synthesis, the pH and temperature were maintained constant at 10 and 60°C, respectively. The preparation took place at room temperature under vigorous stirring. The obtained gel was separated by centrifugation, washed with deionised water and then dried in the oven (80°C) for a further hour before the solid grinding. To synthesise calcined LDH, a thermal treatment in an electric muffle furnace at 500°C for 2 hours was applied under air flow and the obtained product was denoted M_xC500 with x taking a number from 1 to 7.

II.3 Application of the experimental design of mixture for optimizing the layered double hydroxide

The mixture experimental design is a technique to determine the relationship between dependent (response) and independent variables as well as to optimize the relevant processes. Considering Y as a response, x_1, x_2 and x_3 as the independent variables, the response modeling is performed using regression techniques that relate Y to a set of Xi' s factors i.e. $Y = f(x_1, x_2, x_3, \dots \dots x_n)$.

In the present study, three factors were involved in a second-order polynomial model which can be regarded as a good approximation of the interaction and the effects of these variables on the phenomenon studied. The surface response model of the second degree can be written as follows [13]:

$$Y = \sum a_i\, x_i + \sum a_{ij}\, x_i x_j + \varepsilon$$
(1)

Eq. (2)

Where Y is the response variable (% removal ratio of pollutant by adsorption and heterogeneous Fenton-like process) to be modelled, x_i and x_j are the independent variables (the ratio of LDH compositions % Mg, % Cu and % Fe), a_0, a_i, a_{ij} are regression coefficients and ε is the error.

The second degree model for mixture of three factors is written as follows:

$$Y = b_1\, x_1 + b_2\, x_2 + b_3\, x_3 + b_{12} x_1 x_2 + b_{13} x_1 x_3 + b_{23} x_2 x_3 \quad (2)$$

The obtained model should be validated by ANOVA (analysis of variance) which is used to test the adequacy and the significance of each term in the equation (linear and interaction terms) and the goodness of fit of the regression model obtained by the determination of R_{square} and $R_{square\ adjusted}$ [13]. These models use the response surface plots that give information about the main effects and interactions between variables and also their contributions to the response [14]. The results analysis was performed with statistical and graphical analysis software (JMPPRO) which was used to determine the coefficients of regression equation which leads to estimate the optimum points.

II.4 Experimental procedure

Photocatalytic experiments were carried out in a cylindrical batch reactor which had a luminous source (an HPK 125 W Philips ultraviolet lamp with a wavelength maximum of 365 nm), placed in vertical position. The reactor was stirred continuously by a magnetic stirrer.

Photocatalytic degradation experiments were carried out by loading 250 mL of dye solutions in the photocatalytic reactor, then the pH was adjusted by addition of drops of NaOH (0.1and 1M) or HCl (0.1 and 1M). The required amount of photocatalyst and a certain quantity of H_2O_2 were added. All photocatalytic experiments were carried out after three hours of adsorption in the dark. The stability tests were determined by the reused catalyst which was collected and regenerated by washing with water and methanol then dried in the oven.

The dye aqueous solutions of BPv were filtered by use of a Millipore membrane filter, type 0.45 nm, and the concentrations were determined from the UV-vis absorbance characteristic by exploitation of the calibration curve. A Perkin Elmer spectrophotometer was used. The maximum absorption wavelength (λmax) was 637 nm. The ratio quantity of dye elimination was calculated by measuring the concentration of the solution before and after adsorption and photocatalyse, using the following equation:

$$\frac{C_o - C_f}{C_o}\, X\, 100 \qquad \text{Eq. (3)}$$

Where C_0 and C_f are the initial and final (after adsorption or photocatalyse reactions) dye concentrations, respectively.

The effects of different parameters such as the initial the pH, the concentration of catalyst, the amount of oxidant, and the initial concentration of dye, were considered.

II.5 Catalysts characterization:

The materials were characterized by several techniques such as: FTIR, XRD, TG-DTA, particle size distribution, and finally by UV-DRS where the band gap E(eV) was calculated according to the following relationship:

$$E = hC/\lambda \qquad \text{Eq. 4}$$

Eq. (5)

Where h is blank constant = $6.626.10^{-34}$ J.s, C (speed of light) = 3.10^8 ms^{-1}, and λ is cut off wavelength (nm).

III. Results and discussion

III.1 Determination of the optimal layered double hydroxide composition

The response surface methodology (RSM) was used to determine the optimal metal composition of the LDH based on the responses (% removal rate by adsorption and photocatalysis). The obtained results are shown in Table 2.

Table.2 Removal rate for all matrices by adsorption and photocatalysis.

Matrix	Mixture component			Without calcination			Calcined at 500 °C		
	Mg^{2+} (x_1)	Cu^{2+} (x_2)	Fe^{3+} (x_3)	R.R.A (Y)	R.R.P (Y)	R.R.T (Y)	R.R.A (Y)	R.R.P (Y)	R.R.T (Y)
M1	0.45	0.1	0.45	35.13	36.81	60.26	33.90	39.75	60.18
M2	0.45	0.45	0.1	19.34	6.82	19.34	6.32	11.18	20.78
M3	0.1	0.8	0.1	20.25	7.70	25.94	5.26	8.01	12.85
M4	0.33	0.33	0.33	18.45	19.13	31.55	5.47	12.44	17.23
M5	0.8	0.1	0.1	30.85	30.20	50.77	9.85	19.55	27.48
M6	0.1	0.1	0.8	13.19	25.08	32.67	5.12	19.23	23.37
M7	0.1	0.45	0.45	7.62	12.41	16.79	0.512	12.82	13.26

* R.R.A: removal rate by adsorption.

* R.R.P: removal rate by photocatalysis.

* R.R.T: total removal rate.

These results can be used to identify the LDHs which give the highest values of pollutant removal rate to be studied by the two processes, adsorption and photocatalysis (heterogeneous Fenton-like). The transition metals that build the LDH sheets, and the oxides formed from these metals after calcination have a very significant effect on the phenomenon of adsorption and photocatalysis, in this case the statistical analysis and the validation of the models make it possible to study the percentage effect of the Mg^{2+}, Cu^{2+} and Fe^{3+} elements between them as well as their contribution in the optimization of the systems (adsorption and photocatalysis).

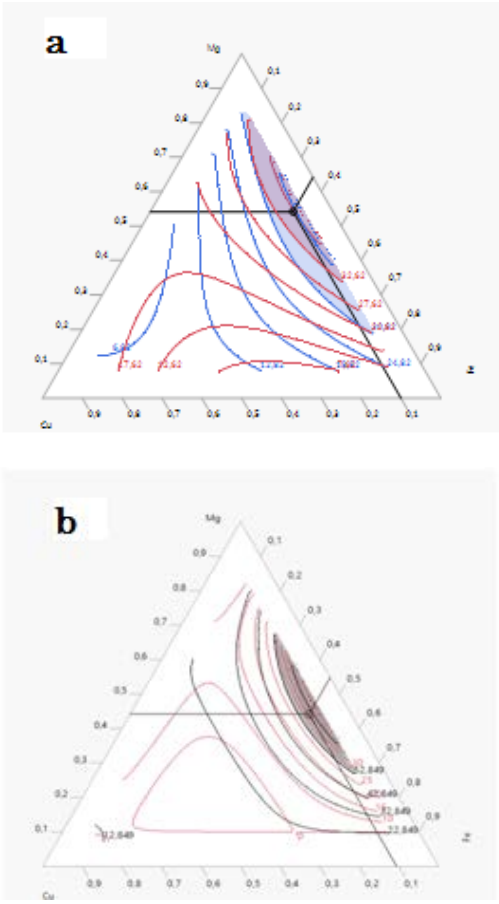

Figure.1 triangular graphic representation of surface response for: (a) NCLDH, (b) LDHC500

The optimum points can be extracted were:

$Mg_{0.54}$-$Cu_{0.1}$-$Fe_{0.36}$-LDH-NC
$Mg_{0.465}$-$Cu_{0.1}$-$Fe_{0.435}$-LDH-C500

III.2 Thermogravimetric analysis

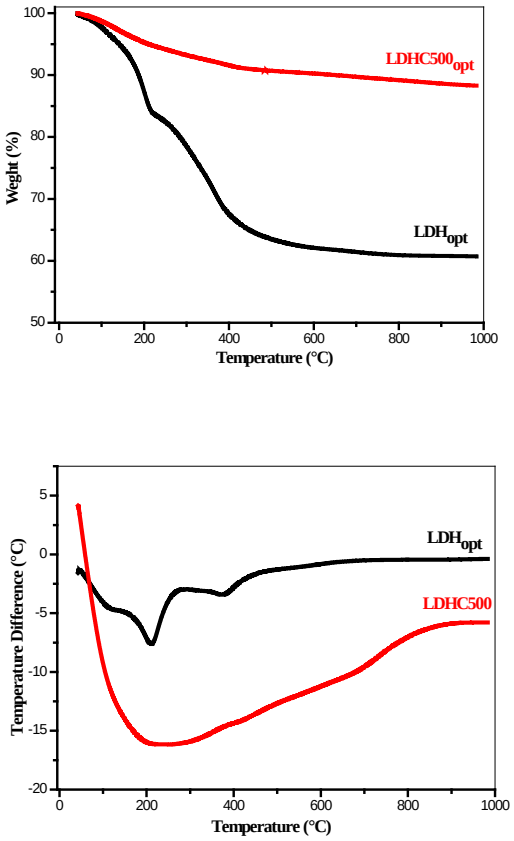

Figure.2 TGA and TDA of LDH_{opt} and $LDHC500_{opt}$

Figure 2 shows the thermal behaviour of the two materials LDH_{opt} and $LDHC500_{opt}$ analysed with TG and TDA. The significant recorded lost weight for the LDH_{opt} (39% in total) in comparison with the $LDHC500_{opt}$ (12% in total) can be seen. That is clear, because it is known that the calcination at 500°C led to the elimination of the major parts of water molecules physi-sorbed and the interlayer water, and caused also the decomposition of the layers, so LDHs lost their typical structure and became oxide metals [15]. Three distinct mass loss consecutive steps were observed for LDH_{opt} sample and two endothermic peaks described by TDA curves appeared at 210 and 376°C, the first one corresponding to the removal of crystallized water and the physi-sorbed water (16%) [16, 17] and the second one ranging from 210 to 376 °C were related to the elimination of the interlayer water (15%) [18]. The third observed stage above 376°C was attributed to the minimum weight loss (8%) which was due to the dehydroxylation and decarbonation, indicating a conversion of OH^- of the brucite-like and CO_3^- in the interlayer to H_2O and CO_2 respectively [19, 20]. For the $LDHC500_{opt}$, two main stages of weight loss could be noted, the first up to 430 °C and the second above 430 °C, and a small weight loss was recorded which might be due to the removal of residual water, hydroxide and carbonate.

III.3 X-ray diffraction (XRD)

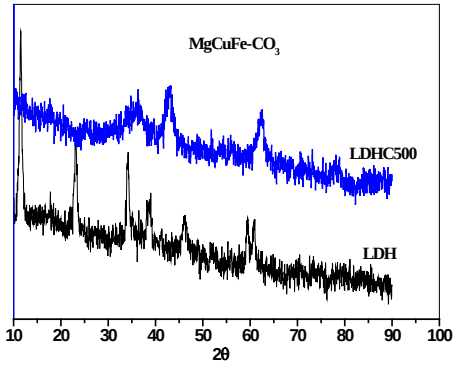

Figure. 3 XRD patterns of LDH_{opt} $LDHC500_{opt}$

Figure 3 shows the XRD patterns of the solid catalyst, LDH_{opt} has two peaks characteristic reflections of the basal (003), (006) and (009) at 2θ around 11.85, 21.1 and 34.1°, respectively. This initial LDH symmetrical reflections show a layered structure [15, 21, 22]. At higher values of 2θ= 60°, a weak non-basal reflections can be observed [21]. While for the calcined LDH ($LDHC500_{opt}$), there was a disappearance of these peaks. *Goh et al* [21] reported that the calcination of LDHs at 500°C destroyed their layer structure and metal oxides would be formed with high thermal stability, large surface area, basic properties, small crystal size, and high stability against sintering even under extreme conditions. ***Sable et al*** **[23]** suggested that the calcination of hydrotalcite at 450°C led to the removal of the NO_x, CO_2 and water. The physi-sorbed water, the interlayer water and the water from the dehydroxylation of the brucite layers could be progressively lost from the LDH calcined at 500 °C **[15]**. After calcination, the crystalline phases of periclase MgO appeared at 43.02° and 62.37° **[24]**.

III.4 SEM/EDX analysis

Table.3 Elemental composition of EDX analysis for LDH_{opt} and $LDHC500_{opt}$

Element	LDH_{opt}		Element	$LDHC500_{opt}$	
	Weight %	Atomic %		Weight %	Atomic %
Cl K	0.315	0.19	Zn K	0.5525	0.1675
C K	11.236	21.544	O K	50.778	62.962
O K	34.148	52.862	Si K	0.28	0.2
Zn K	0.734	0.318	C K	12.24	18.52
Al K	0.48	0.68	Mg K	15.612	12.856
Nb L	1.52	0.35	Cu K	4.504	1.418
Mg K	20.91	17.067	Fe K	18.704	6.718
Cu K	5.62	2.502			
Fe K	30.29	13.817			

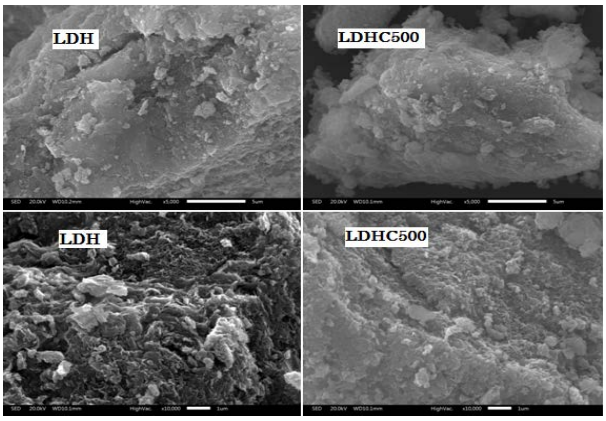

Figure.4 SEM image of LDH_{opt} and $LDHC500_{opt}$

The surface morphology of LDH_{opt} and $LDHC500_{opt}$ and their derivatives was examined by SEM, which shows in Fig. 4 that the particles appeared almost irregular in shape and size, this morphology is typical of double layered hydroxides prepared by co-precipitation method [**19**]. The SEM micrograph (Fig. 4) LDH and LDH calcined at 500°C showed significant difference in surface morphology, which means that calcination at 500°C affected the external morphology of LDH.

Tab.3 shows the mean of the elementary concentrations of the metal cations on the surface of LDH calculated by the EDS-SEM technique in several surface spots. These cations should play an essential role in the catalytic activity **[25],** in the other hand the ratio of these metal cations gives an important information about LDH structure **[26]**. The EDS curves of LDH_{opt} showing the presence of Mg, Cu, Fe, O and C, and traces of Cl, Zn and Al, The presence of Cl probably originated from the initial precursor of preparation ($MgCl_2$, $CuCl_2$ and $FeCl_3$) which were not eliminated, the presence of C and O was clearly due the intercalation by carbonates CO_3^{2-} and air. The results illustrated on Table 3 show that the Mg, Fe, Cu, O and C were well distributed on the surface of the powder of LDH_{opt}. The masse ratio of Mg, Cu and Fe is 30.29, 5.62 and 17.42% respectively, which were approximately the same molar ratio of the initial precursors used for the preparation of the optimum LDH (Mg: 0.54, Cu: 0.1, Fe: 0.44). The XRD pattern and chemical analysis result confirmed that the layered structure material containing Cu^{2+}, Mg^{2+}, Fe^{3+} and with CO_3^{2-} in the interlayer had been successfully synthesized. in the case of LDH calcined at 500 °C, the major elements appearing in the EDS spectrum were Mg, Cu, Fe, O, and C, and slightly traces of Si and Zn, the average ratio masse of the composition of $LDHC500_{opt}$, Mg = 18.7%, Cu = 4.5 % and finally Fe = 15.61%. These results showed clearly the dispersion of these cations on the surface of solid and confirmed the initial values of precursors used for the preparation of the LDHC500 optimum (Mg: 0.46, Cu :0.1, Fe :0.44).

III.5 UV-DRS

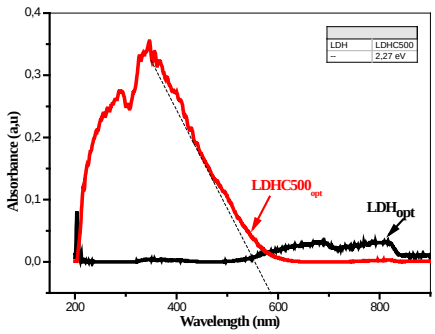

Figure.5 UV-Vis diffuse reflectance spectra of LDH_{opt}, $LDHC500_{opt}$

As shown in Fig. 5, no significant band absorption for LDH_{opt} could be observed. This is means that LDH_{opt} was optically transparent, in agreement with the work of *Zhou et al* [27], while the material $LDHC500_{opt}$ could absorb the visible-light wave length, especially below of 500 nm. This was probably due to the formation of oxide metals, such as Fe_2O_3, CuO…, which were photo catalytically active in visible light. In the other hand, the band gap of $LDHC500_{opt}$ was estimated to be 2.27; these values were almost equal to results found in [29] which indicated the formation

of CuO and $CuFe_2O_4$. The increase in band gap lets suggested that $LDHC500_{opt}$ might have greater catalytic activity for visible light **[30]**.

III.6 pH Effect on the photocatalytic degradation of BPv

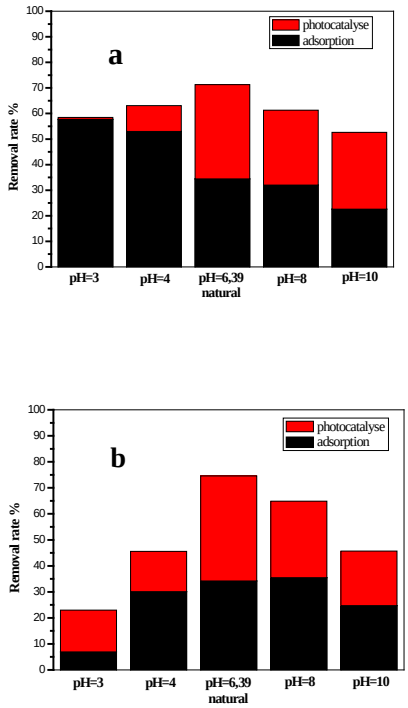

Figure.6 pH effect on the BPv removal by adsorption and photocatalysis (a) LDH_{opt}, (b) $LDHC500_{opt}$,

The pH of solution is an important factor on the adsorption of the organic compounds, and become more crucial in the photocatalytic reactions containing transition metals (Fe, Cu…). Fig. 6 shows the effect of pH value on the removal of BPv in dark and under UV light. The experiments were carried out at pH within the range 3-10 at 0.05 g L^{-1} dye concentration and 0.5 g L^{-1} photocatalyst loading. In the case of LDH_{opt}, the results showed that the rate of adsorption decreased with the increasing of pH, on the other hand for the photocatalysis, the removal rate increased with increasing pH up to the maximum value at pH (natural) = 6.39 (37%). While for the $LDHC500_{opt}$, the efficient removal of BPv by adsorption and photocatalysis was near the pH natural (6.39) and pH= 8. The surface was negatively charged at pH above pH_{pzc} (witch equal 8.53, 8.77 for LDH_{opt} and $LDHC500_{opt}$ respectively) and positively charged at pH less than these values, for this reason the BPv anions were attracted to adsorption sites of LDH at pH<pH_{pzc}. This phenomenon was not observed after calcination because LDHs lost their characterisation by the formation of metal oxides on their surfaces. The degradation efficiency of BPv by LDH increased with increasing of pH until pH natural= 6.39 (37 %). It is known that Fenton reaction is enhanced at pH < 4 by the contribution of the homogenous process due to Fe^{3+} leaching, but in this case it can be seen that photocatalyse at pH acid (3 and 4) illustrated a weak removal ratio (3% and 10 %) respectively. These results were probably due to a low concentration of the iron in solids (17.42% in the weight of catalyst) and the weak Fe leaching. Therefore, the activity catalytic performance was more important in the alkaline medium for non calcinated and calcined LDH; this phenomenon maybe related copper species that contain LDH because Cu led to the acceleration of the generation of $OH^{\bullet}$ radicals in a wide range of pH **[31]**. Similar results were obtained for the products contain a copper as active species used in the photocatalytic reaction **[32]**.

III.7 Effect of initial dye concentration

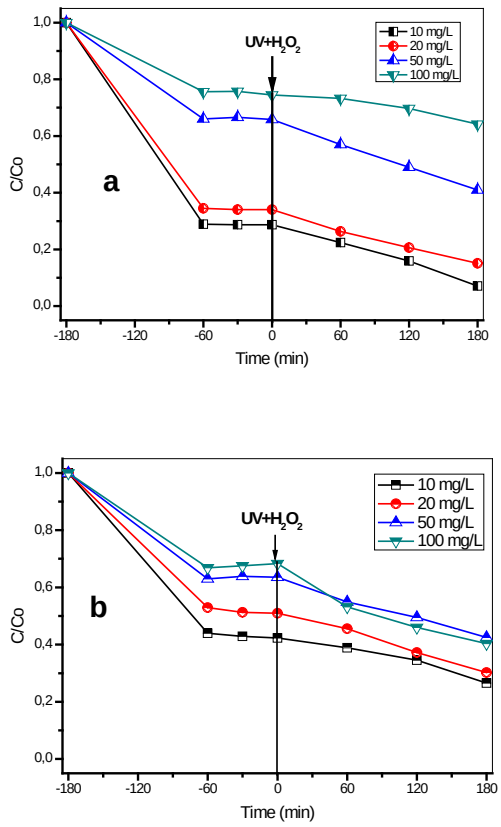

Figure.7 dye initial concentration effect on the degradation efficiency by the photo catalysts (a) LDH_{opt} and (b) $LDHC500_{opt}$

The effect of the initial dye concentration on the degradation rate by the heterogeneous Fenton systems ($LDH_{opt}/H_2O_2/UV$, $LDHC500_{opt}/H_2O_2/UV$) was investigated using different concentrations of BPv of 10, 20, 50 and 100 $mg.L^{-1}$, and other parameters such as the pH, the catalyst dose, the concentration of H_2O_2 remained constant at 6.34, 0.5 g $.L^{-1}$ and 15.8 mM, respectively, in a solution of 250 mL to which H_2O_2 was added and the UV lamps were lighted up after three hours for the adsorption and desorption equilibrium to be reached. In the case of LDH_{opt}, it is clear that the rate of degradation decreased by increasing the concentration of dye as shown in Fig. 7. This reduction was probably due to an insufficient concentration of free radicals compared to a large amount of available pollutants molecules. In addition, a high concentration of dye could prevent the photons from arriving at the active sites by forming an internal filter thus allowing participation in the photocatalysis reaction. On the other hand, a large quantity of the organic molecules which had been adsorbed by the material could occupy the active sites, leading to the reduction of the performance catalysts **[33].** In the other hand, no significant difference was observed about the BPv degradation rate with the difference concentration for the $LDHC500_{opt}$. As known, the calcination changed the surface morphology of materials by the destroying the layers and the formation of transition metal oxides, so it can be suggested that the mechanism of photocatalytic degradation changed, and the dye concentration had not significant effect on the photocatalyse performance.

III.8 Effect of photocatalyst dose

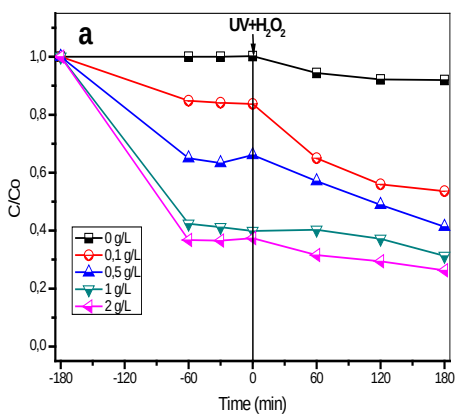

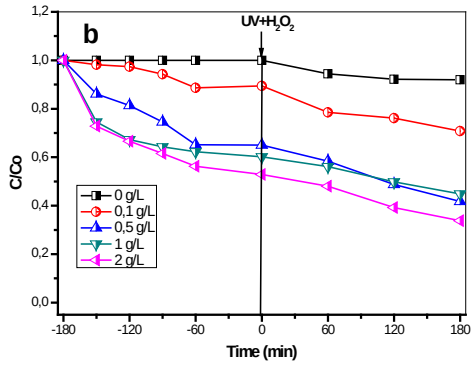

Figure.8 photocatalyst dose effect on the degradation efficiency by the photo catalysts (a) LDH_{opt}, (b) $LDHC500_{opt}$

The effect of catalyst dose on the BPv degradation was studied by varying the amount of catalyst from 0.1 to 2 $g.L^{-1}$ at pH = 6.4, the concentration of H_2O_2 was fixed at 15.8 mM and the solution exposed to UV irradiation after stirring vigorously for three hours in black to achieve an adsorption/desorption equilibrium. It can be observed in Figure 8 that the removal of BPv by adsorption onto LDH_{opt} and $LDHC500_{opt}$ was enhanced with the catalyst dosage increasing. This increased molecules adsorption due to the increase of adsorption sites. The degradation rate via photocatalysis increased with increasing of catalyst dose until an optimum value with a catalyst dose equal 0.5 $g.L^{-1}$ in all systems studied. An increase in the catalyst concentration normally improved the formation of free radicals $OH^{\bullet}$, consequently led to increasing of degradation rate due to availability of free active sites on the surface area [33]. Beyond this optimal value of LDH_{opt} the decrease in the removal rate is explained by the fact that the turbidity of the treated solution increased due to the increase of the catalyst mass, so the penetration of the photons was strongly reduced within the liquid, hence the total number of photons that could react with H_2O_2 decreased [34]. In the other hand, an excessive Fe and Cu species dissolved from catalyst could be presented as scavenger elements, according to the following equations [34-36]:

$$OH^{\bullet} + Fe^{2+} \rightarrow OH^{-} + Fe^{3+}$$
(5a)

Eq. (6)

$$Cu^{+} + OH^{\cdot} \rightarrow Cu^{2+} + OH^{\bullet}$$ (5b) Eq. (7)

III.9 Effect of initial H_2O_2 concentration

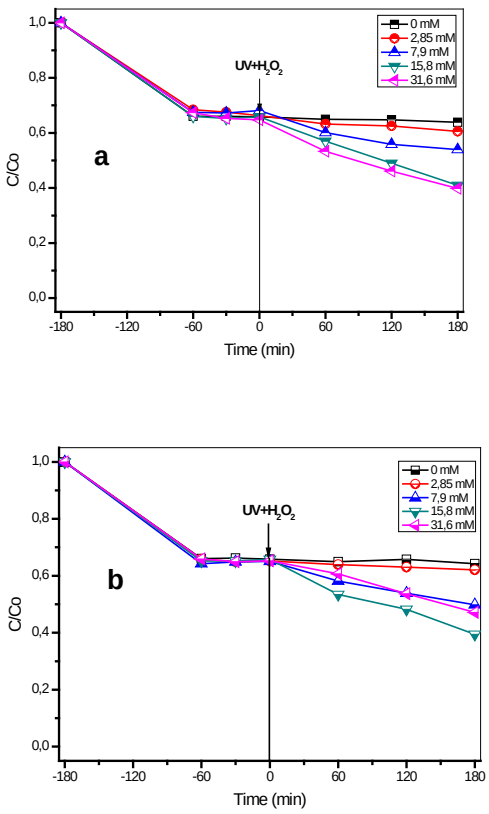

Figure. 9 H_2O_2 initial concentration effect on the degradation efficiency by the photo catalysts (a) LDH_{opt}, (b) $LDHC500_{opt}$

H_2O_2 was an important parameter for the degradation of organic molecules in the heterogeneous Fenton-like system because it was considered as a precursor of free radicals. The degradation of BPv by the heterogeneous Fenton-like method using photo catalysts LDH_{opt} and $LDHC500_{opt}$ was studied with different concentrations of H_2O_2 ranging between 2.85 mM and 63.2 mM. The obtained results are illustrated in Fig. 9.

The required stoechiometric amount of H_2O_2 for complete mineralization of 50 mg L^{-1} of BPv was 2.85 mM calculated according to the following oxidation reaction:

$$C_{27}H_{36}CaN_2O_7S_2 + 32H_2O_2 \rightarrow 26CO_2 + 2H_2O + 2H_2SO_4 + 2HNO_3 + CaCO_3 + 90\,H^+ + 90e^- \quad (6)$$

Eq. (8)

Without H_2O_2, no degradation of the BPv occurred during three hours of photodegradation as shown in Figure 9. The obtained results show that the degradation of BPv was accelerated with H_2O_2 concentration increasing from 2.85 to 15.8 mM after it could be observed that the addition of H_2O_2 decreased the photocatalytic performance as expected. The beneficial effect of the presence of H_2O_2 could be attributed to the increase in the concentration of free radicals generated by the photolytic peroxidation of H_2O_2, according to the equation:

$$H_2O_2 + hv \rightarrow 2OH^\bullet \quad (7)$$

Eq. (9)

The decrease of degradation efficiency of BPv above of 15.8 mM of H_2O_2 concentration was probably due to a scavenging effect of H_2O_2, which can be presented by equations [37, 38]:

$$H_2O_2 + HO^\bullet \rightarrow H_2O + HO_2^\bullet \quad (8)$$

Eq. (10)

$$HO_2^\bullet + HO^\bullet \rightarrow H_2O + O_2 \quad (9)$$

Eq. (11)

The optimum value of initial concentration of H_2O_2 in the degradation of BPv was 15.8 mM, higher than the theoretical value given above. It can be suggested that the reason of this was due to the evaporation of H_2O_2 and to parallel H_2O_2 consuming reactions [39]:

$$\equiv Fe^{3+} + H_2O_2 \rightarrow \equiv Fe^{2+} + HO_2^\bullet \quad (10)$$

Eq. (12)

$$\equiv Cu^{2+} + H_2O_2 \rightarrow \equiv Cu^{+} + HO_2^\bullet + OH^- \quad (11)$$

Eq. (13)

So the real amount which reacted in the solution was very much less than that of the added H_2O_2.

III.10 Catalyst stability and reusability

In order to evaluate the stability and cost-effectiveness of the LDH_{opt} and $LDHC500_{opt}$ catalysts considered in this work, they were reused in three consecutive reactions, maintaining the same operating conditions. After each use, the catalyst was washed with water several times. The obtained results are presented in Figure 10.

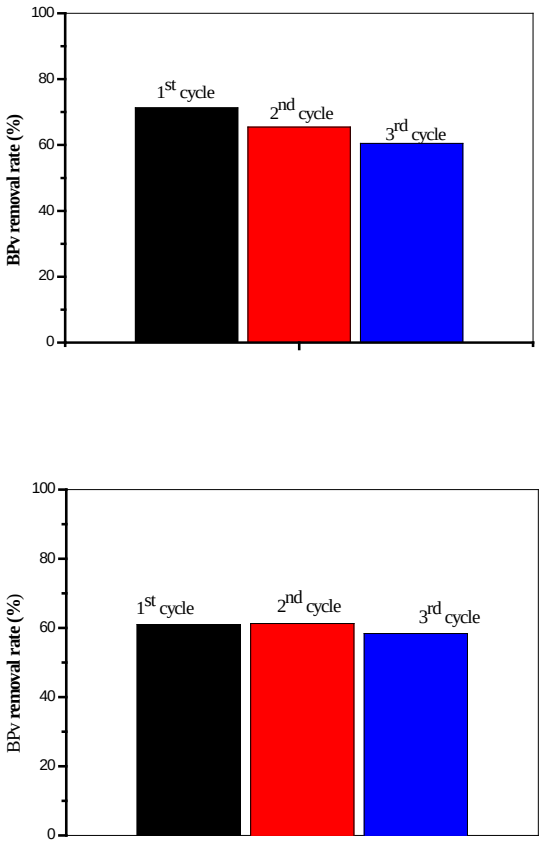

Figure.10 Reuse and stability of catalyst

As shown in Fig. 10 the photo catalysts conserved their performance for the photocatalytic efficient after calcinations, this is may be due to the formation of metal oxide on the surface.

IV. Conclusion

This paper describes the optimisation synthesis and characterization of layered double hydroxide and their derivatives. Its application in the heterogeneous Fenton-like was investigated. The XRD patterns confirmed the layered structure of LDH, while after the calcination this material lost its initial structure. The distribution of size particles analysis demonstrated that there was an amelioration of cristallinity after thermal treatment at 500°C. The UV diffuse reflectance spectroscopy analysis showed that LDH was photo catalytically inactive; LDHC500 could absorb the visible-light wave length, especially below of 500 nm. This study demonstrated a significant effect of the experimental parameters such as pH, initial dye concentration, catalyst loading, and H_2O_2 concentration. The applicability of heterogeneous Fenton like process for the elimination of organic pollutant at neutral pH have a strong advantage, because it avoids the iron and copper leaching which makes possible for the catalysts to have long term stability and no iron sludge formation. This work shows that an organic pollutant can be eliminated by a low cost material, simple to synthesis and to use in the Fenton-like process.

V. References

1. R. R. Dalbhanjan, N. S. Pande, B. P. Shrut, H. V. Ashish, P. R. Gogate, M. R. Gogate, Degradation of patent blueV dye using modified photocatalytic reactor based on solar and UV irradiations, Desalination and Water Treatment, (2015) 1–12.

2. N Barka, S Qourzal, A Assabbane, A Nounah, Y Ait-Ichou, Photocatalytic degradation of patent blue V by supported TiO_2: kinetics, mineralization, and reaction pathway, Chemical Engineering Communications, 198 (2011) 1233–1243.

3. Executive Decree No. 14-212 of 15 May 2012, Official journal of Algeria,

4. M. Lucová, J. Hojerová, S. Pazoureková, Z. Klimová, Absorption of triphenylmethane dyes Brilliant Blue and Patent Blue through intact skin, shaven skin and lingual mucosa from daily life products, Food and Chemical Toxicology, 52 (2013) 19–27

5. V. Vaiano, G. Iervolino, D. Sannino, J. J. Murcia, M. C. Hidalgo, P. Ciambelli, J. A. Navio, Photocatalytic removal of Patent Blue V dye on Au-TiO2 and Pt-TiO2 catalysts, Applied Catalysis B: Environmental, 188 (2016) 1-37

6. E. S. Elmolla, M. Chaudhuri, Comparison of different advanced oxidation processes for treatment of antibiotic aqueous solution, Desalination 256 (2010) 43-47.

7. M, Munoz, Z. M. de Pedro, J. A. Casas, J. J. Rodriguez, Preparation of magnetite-based catalysts and their application in heterogeneous Fenton oxidation - review, Applied Catalysis B, Environmental, 176 (2015) 1-54

8. H. Tekin, B. Okan, S. A. Selale, H. B. Tolga, C. Haluk, F. Dilek Sanin, B. D. Filiz, Y Ulku, Use of Fenton oxidation to improve the biodegradability of a pharmaceutical wastewater, Journal of Hazardous Materials, 136 (2006) 258-265.

9. N. Dulova, T. Marina, D. Aleksander, Catalytic degradation of picric acid by heterogeneous Fenton-based processes, Environmental Technology, 32 (2011) 439-446.

10. W. T. Reichle, Synthésis of anionic clay minerals (mixed metal hydroxides, hydrotalcite), Solid States Ionics, 22 (1986) 135-141.

11. F Bruna, R Celis, I Pavlovic, C Barriga, J Cornejo, M.A Ulibarri, Layered double hydroxides as adsorbents and carriers of the herbicide (4-chloro-2-methylphenoxy) acetic acid (MCPA): Systems Mg–Al, Mg–Fe and Mg–Al–Fe, Journal of Hazardous Materials,168 (2009) 1476-1481.

12 R. Mrad, R. Cousin, C. Poupin, A. Aboukaïs, S Siffert, Propane oxidation and NO reduction over MgCu–Al(Fe) mixed oxides derived from hydrotalcite-like compounds, Catalysis Today, 257 (2015) 98–103

13. M. Ghaedi, H. Zare Khafri, A. Asfaram, A. Goudarzi, Response surface methodology approach for optimization of adsorption of Janus Green B from aqueous solution onto ZnO/Zn (OH)2 –NP-AC: Kinetic and isotherm study, Spectrochimica Acta Part A: Molecular and Biomolecular Spectroscopy, 152 (2015) 233-40

14. A. Asfaram, M. Ghaedi, A. Goudarzi, M. Rajabi, Response surface methodology approach for optimization of ultrasound-assisted removal for simultaneous dyes and ions onto Mn doped Fe3O4-NPs loaded on AC: Kinetic and isotherm study, Dalton Transactions, 44 (2015)14–23

15. Y. Guo, Z. Zhu, Y. Qiu, J. Zhao, Enhanced adsorption of acid brown 14 dye on calcined Mg/Fe layered double hydroxide with memory effect, Chemical Engineering Journal, 219 (2013) 69–77

16. B. Li, S. Yuan, Synthesis, characterization, and evaluation of Ti Mg Al Cu mixed oxides as novel SOx removal catalysts, Ceramics International, 40 (2014) 11559– 11566

17. A. Clearfield, M. Kiek, J. Kwan, J.L. Colon, R.C. Wang, Intercalation of dodecyl sulphate into layered double hydroxide, journal of inclusion phenomena and molecular recognition in chemistry, 11 (1991) 361-378

18. K. S. Abou-El-Sherbini, I. M. M. Kenawy, M. A. H. Hafez, H. R. Lotfy, Z. M.E.A. AbdElbary, Synthesis of novel CO_3^{2-}/Cl^-bearing 3(Mg + Zn)/(Al + Fe) layered double hydroxides for the removal of anionic hazards, Journal of Environmental Chemical Engineering, 777 (2015) 1-15

19. Y. Kuang, L. Zhao, S. Zhang, F. Zhang, M. Dong, S. Xu, Morphologies, Preparations and Applications of Layered Double Hydroxide Micro-Nanostructures, Materials, 3 (2010) 5220-5235

20. K.M. Parida, L. Mohapatra, Carbonate intercalated Zn/Fe layered double hydroxide: A novel photocatalyst for the enhanced photo degradation of azo dyes, Chemical Engineering Journal, 179 (2012) 131–139

21. K-H. Goha, T-T. Lima, Z, Dong, Application of layered double hydroxides for removal of oxyanions: A review, Water research, 42 (2008) 1343 – 1368

22. R. Shan, L. Yan, Y. Yang, K. Yang, S. Yu, H. Yu, B. Zhu, B. Du, Highly efficient removal of three red dyes by adsorption onto Mg–Al-layered double hydroxide, Journal of Industrial and Engineering Chemistry, 21 (2015) 561–568

23. S. S. Sable, F. Medina, S. Contreras, Clofibric acid degradation by catalytic ozonation using hydrotalcite-derived catalysts, Applied Catalysis B: Environmental, 150–151 (2014) 30–36

24. X. Lin, R. Li, M. Lu, C. Chen, D. Li, Y. Zhan, L. Jiang, Carbon dioxide reforming of methane over Ni catalysts prepared from Ni–Mg–Al layered double hydroxides: Influence of Ni loadings, Fuel, 162 (2015) 271-280

25. G. Hannah, Layered Double Hydroxides: Structure, Synthesis and Catalytic Applications, Doctoral thesis, (2012), University of Huddersfield.

26. S. Myata, anion exchange properties of hydrotalcite-like compounds, clays and clay minerals, 31 (1983) 305-311

27. Y. Zhou, L. Shuai, X. Jiang, F. Jiao, J. Yu, Visible-light-driven photocatalytic properties of layered double hydroxide supported-Bi_2O_3 modified by Pd (II) for methylene blue, Advanced Powder Technology, 26 (2015) 439-447

28. K. Ramachandran, S. Chidambaram, B. Baskaran, A. Muthukumarasamy, G. M. Kumar, One pot polyol synthesis of CuO $CuFe_2O_4$ nanocomposites and their

structural, optical and electrical property studies, Materials Letters 175 (2016) 106-109

29. S. Xi, L. Zhang, X. Zhou, G. Pan, Z. Ni, The photocatalytic property for water splitting and the structural stability of Cu Mg M layered double hydroxides (M = Al, Cr, Fe, Ce), Applied Clay Science, 114 (2015) 577-585

30. J. Herney-Ramirez, A. V. Miguel, M. M. Luis, Heterogeneous photo-Fenton oxidation with pillared clay-based catalysts for wastewater treatment : A review, Applied Catalysis B: Environmental, 98 (2010) 10-26.

31. Y. Zhan, H. Li, Y. Chen, Copper hydroxyphosphate as catalyst for the wet hydrogen peroxide oxidation of azo dyes, Journal of Hazardous Materials, 180 (2010) 481-485

32. P. R. Chowdhury and K. G. Bhattacharyya, Ni/Ti layered double hydroxide: Synthesis, characterization and application as a photocatalyst for visible light degradation of aqueous methylene blue, Dalton Transactions, 44 (2015) 21-24

33. M.B. Kasiri, H. Aleboyeh, A. Aleboyeh. Degradation of Acid Blue 74 using Fe-ZSM5 Zeolite as a heterogeneous photo-Fenton catalyst. Applied Catalysis B: Environmental. 84 (2008) 9-15.

34. X. Zhang, Y. Ding, H. Tang, X. Han, L. Zhu, N. Wang, Degradation of bisphenol A by hydrogen peroxide activated with $CuFeO_2$ microparticles as a heterogeneous Fenton-like catalyst: Efficiency, stability and mechanism, Chemical Engineering Journal, 236 (2014) 251-262

35. M. Idrissi, Y. Miyah, Y. Benjelloun, M. Chaouch, Degradation of crystal violet by heterogeneous Fenton-like reaction using Fe/Clay catalyst with H_2O_2, Journal of Material and Environment Sciences, 7 (2016) 50-58

36. S. Kumar, M. A. Isaacs, R. Trofimovaite, L. Durndell, C. M.A. Parlett, R. E. Douthwaite, B. Coulson, M. C.R. Cockett, K. Wilson, A. F. Lee, P25@CoAl layered double hydroxide heterojunction nanocomposites for CO_2 photocatalytic reduction, Applied Catalysis B: Environmental, 209 (2017) 394-404

37. L. Wang, D. Li, H. Watanabe, M. Tamura, Y. Nakagawa, K. Tomishige, Catalytic performance and characterization of Co/Mg/Al catalysts prepared from hydrotalcite-like precursors for the steam gasification of biomass, Applied Catalysis B: Environmental, 150–151 (2014) 82–92

38. H. Chen, Z. Zhang, Z. Yang, Q. Yang, B. Li, Z. Bai, Heterogeneous Fenton-like catalytic degradation of 2,4-dichlorophenoxyacetic acid in water with FeS, Chemical Engineering Journal, 273 (2015) 481-489

39. Y. Wang, H. Zhao, G. Zhao, Iron-copper bimetallic nanoparticles embedded within ordered mesoporous carbon as effective and stable heterogeneous Fenton catalyst for the degradation of organic contaminants, Applied Catalysis B: Environmental, 164 (2015) 396-406